

# Appearance Decomposition and Reconstruction of Textured Fluorescent Objects

Shoji Tominaga, Keiji Kato, Keita Hirai, Takahiko Horiuchi

Graduate School of Advanced Integration Science, Chiba University, Chiba, Japan

## Abstract

This paper analyzes the surface appearance of a textured fluorescent object. First, the bispectral radiance factor of the fluorescent object is decomposed into the fluorescent emission (luminescent) component and the reflection component, which are summarized as the Donaldson matrix. Second, the observed spectral images are described by a multiplication of two factors: one factor is spectral functions depending on wavelength and another is the weighting factors representing the surface texture. An algorithm is proposed to estimate the bispectral functions and the location weights from the spectral images observed under multiple illuminants. Third, the two textured images of the reflection component and the luminescent component are constructed using the estimates of the spectral function and the location weights. Also the surface appearances of the same fluorescent object under arbitrary illumination are constructed by combining the two component images.

## Introduction

Fluorescent materials are used in painted objects, papers, plastics, clothes, and all sorts of things that we may come across each day. Fluorescence is a luminosity phenomenon where a material is first excited by light radiation in a specific wavelength region, and then the excited state relaxation emits light radiation in another longer wavelength region [1],[2]. Many fluorescent objects appear brighter and more vivid than the original object color based on a non-fluorescent light reflection. The fluorescent characteristics are described in terms of the bispectral radiance factor. The radiance factor is a function of two wavelength variables: the excitation wavelength of incident light and the emission/reflection wavelength. The bispectral radiance factor can be summarized as a Donaldson matrix [3], which is an illuminant independent matrix representation of the bispectral radiance factor of a target object.

The bispectral radiance factor can be measured using two monochromators normally. Traditionally, standard procedures for using two monochromator methods were proposed by the CIE [4], and several standardization and accuracy in fluorescent radiance measurement were discussed in various fields [5]-[8]. The two-monochromator method is precise and direct in order to measure the bispectral radiance factor. However, an essential problem of the two-monochromator method is time-consuming and expensive, which is confined in the laboratory setup.

We proposed a method for estimating the bispectral Donaldson matrices of fluorescent objects by using only two illuminant projections [9]. We also discussed the mutual illumination phenomenon between two fluorescent objects [10]-[12]. By knowing the Donaldson matrices, appearances of the fluorescent objects are reconstructed under different illuminations [13]. In the previous studies, we supposed that the fluorescent

objects had only smoothed matte surfaces and the illumination was uniform. However, we note that the perceived texture of the image includes not only surface texture but also the non-uniformity and shading effect by illumination conditions. Also, most material surfaces are not always smoothed but have some uneven texture such as irregularities, roughness, and patterns

In this paper we analyze the surface appearance of a fluorescent object with textures by surface geometries and roughness. We describe the bispectral radiance factor of the fluorescent object by the Donaldson matrix. First, we show that the observed spectral image are modeled by a multiplication of two factors of the spectral functions depending on wavelength and the location weights representing the texture information of the surface. Second, a nonlinear algorithm is proposed to estimate the spectral reflectance, the bispectral luminescent radiance factor, and the texture information at each pixel point. Third, the observed image is decomposed into two textured images of the reflection component and the luminescent component. The surface appearances of the textured fluorescent object under arbitrary illumination can be constructed by combining the two component images.

## Bispectral Properties of Fluorescent objects

The bispectral properties of a fluorescent object can be explored using two monochromators, where one is placed in the irradiating beam and the other is placed in the viewing beam. Let  $\mathbf{D}$  be a Donaldson matrix representing the tabular form of complete bispectral radiance factor  $D(\lambda_{em}, \lambda_{ex})$ . The excitation wavelength  $\lambda_{ex}$  corresponds to one direction in the array and the emission wavelength  $\lambda_{em}$  corresponds to the other direction. Figure 1 illustrates the Donaldson matrix of a yellow paint containing a fluorescent color [9].

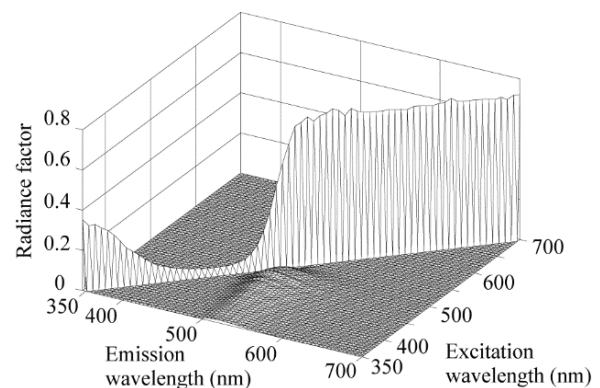


Figure 1. Bispectral Donaldson matrix obtained from a yellow paint containing a green fluorescent color.

The Donaldson matrix was measured with our bispectrometer system in the range [350, 700nm] with 5nm intervals, where monochromatic light corresponding to each excitation wavelength was projected on the surface in 5nm step. Figure 1 shows a  $71 \times 71$  square array of the matrix of bispectral radiance factor. The diagonal represents the reflected radiance factor that produces yellow color. The reason of why the matrix is triangular and the luminescent component is located only in the lower half of the off-diagonal is that the luminescent energy is emitted at longer wavelength than each excitation wavelength. This shift of off-diagonal is called Stokes shift [2].

In Figure 1, a hump in the range [500, 600nm] of emission wavelength represents the luminescent radiance factor. The spectral radiance factor  $D_L(\lambda_{em}, \lambda_{ex})$  is a function of both emission and excitation wavelengths. We can assume that the luminescent radiance factor can be separated into the emission and excitation wavelength components as  $D_L(\lambda_{em}, \lambda_{ex}) = \alpha(\lambda_{em})\beta(\lambda_{ex})$ . A general form of the Donaldson matrix  $\mathbf{D}$  with the above properties can be represented in an  $N \times N$  matrix as

$$\mathbf{D} = \mathbf{D}_R + \mathbf{D}_L$$

$$= \begin{bmatrix} s_1 & 0 & \cdots & 0 \\ 0 & s_2 & \ddots & \vdots \\ \vdots & \ddots & \ddots & 0 \\ 0 & \cdots & 0 & s_N \end{bmatrix} + \begin{bmatrix} 0 & \cdots & \cdots & 0 \\ \alpha_2\beta_1 & 0 & & \\ \alpha_3\beta_1 & \alpha_3\beta_2 & 0 & \\ \vdots & \vdots & \ddots & \ddots \\ \alpha_N\beta_1 & \alpha_N\beta_2 & \cdots & \alpha_N\beta_{N-1} \end{bmatrix}, \quad (1)$$

where  $(i = 2, 3, \dots, N)$ ,  $(i = 2, 3, \dots, N)$ , and  $(i = 2, 3, \dots, N-1)$  represent, respectively, the reflected radiance factor corresponding to surface-spectral reflectance, the emission spectrum, and the excitation spectrum.

## Observation Model

Let us suppose that a fluorescent object with matte surface is illuminated uniformly with a single light source. Let  $S(\lambda)$ ,  $\alpha(\lambda)$ , and  $\beta(\lambda)$  be the continuous functions of the surface-spectral reflectance, the emission spectrum, and the excitation spectrum of the object, respectively. Also let  $E(\lambda)$  be the illuminant spectrum of the light source. We suppose that the object surface is not necessarily smooth but a textured rough surface.

The observations of spectral radiances at location  $\mathbf{x}=(x, y)$  of the object surface are described as

$$y(\mathbf{x}, \lambda_{em}) = f_1(\mathbf{x})S(\lambda_{em})E(\lambda_{em}) + f_2(\mathbf{x})\alpha(\lambda_{em}) \int_{350}^{\lambda_{em}} \beta(\lambda_{ex})E(\lambda_{ex})d\lambda_{ex}$$

$$= f_1(\mathbf{x})S(\lambda_{em})E(\lambda_{em}) + f_2(\mathbf{x})\alpha(\lambda_{em})C(\lambda_{em}) \quad (2)$$

where the interval of integration is  $[350, \lambda_{em}]$  because the excitation starts from about 350nm. The weights  $f_1(\mathbf{x})$  and  $f_2(\mathbf{x})$  to the spectral functions are variable of location  $\mathbf{x}$  and independent of wavelength  $\lambda$ . The location weights represent the texture information of the surface. The two terms in Eq.(2) represent,

respectively, the diffuse reflection component and the fluorescent emission component.

We can summarize the observation model in matrix form. Let  $\mathbf{s}$ ,  $\boldsymbol{\alpha}$  and  $\mathbf{e}$  be  $N$ -dimensional column vectors representing the reflectance, emission, and illuminant spectra, respectively. Also, let  $\mathbf{f}(\mathbf{x})$  be two-dimensional column vector representing the location weights, that is, the texture information, and  $\mathbf{A}$  be an  $N \times 2$  matrix as follows:

$$\mathbf{A} = [\mathbf{s} \circ \mathbf{e} \quad \mathbf{c} \circ \boldsymbol{\alpha}], \quad (3)$$

$$\mathbf{f}(\mathbf{x}) = [f_1(\mathbf{x}) \quad f_2(\mathbf{x})]^t$$

where symbols  $\circ$  and  $t$  represent element-wise multiplication and matrix transposition, respectively. Then the observations are then modeled in a simple matrix equation as

$$\mathbf{y}(\mathbf{x}) = \mathbf{A}\mathbf{f}(\mathbf{x}). \quad (4)$$

## Estimation Algorithm of Spectral Functions and Location Functions

The Donaldson matrix is composed of the surface-spectral reflectance component in the diagonal and the luminescent component in the off-diagonal. The luminescent component is further decomposed into the emission and excitation spectral components. We consider that the target fluorescent object has a specific Donaldson matrix, and the weighted matrix is observed at each pixel point. The weighting coefficient is variable of location, which represents the surface texture. We should note that the bispectral functions and the two-dimensional location weighting functions are independent of illuminant.

We develop a method to estimate the two unknown factors: the bispectral functions and the location functions from the observed spectral images of a fluorescent object. This estimation leads to a nonlinear estimation problem to minimize a residual error  $\|\mathbf{y} - \mathbf{A}\mathbf{f}\|^2$ , because both  $\mathbf{A}$  and  $\mathbf{f}$  are unknown in Eq.(4), even though the illuminant  $\mathbf{e}$  is given. This paper proposes an iterative approach to solve this nonlinear estimation problem. The unknown quantities to be estimated are the spectral functions  $S(\lambda)$ ,  $\alpha(\lambda)$ ,  $\beta(\lambda)$  and the location functions  $f_1(\mathbf{x})$  and  $f_2(\mathbf{x})$ . We note here that the wavelength range of fluorescent emission  $\beta(\lambda)$  is narrow, and can be measured by using a separate way such as the use of a UV light source. So we assume that the wavelength range of  $\beta(\lambda) > 0$  is given. Moreover, we assume that the texture is based on surface roughness, and the averages of the location weights over the entire surface are one as  $E[\mathbf{f}(\mathbf{x})] = [1 \quad 1]^t$ .

Our iterative approach is based on an alternate estimation of the spectral functions and the location weights. Instead of the joint minimization over variables  $\lambda$  and  $\mathbf{x}$ , we separate the minimization into two steps of a linear least squares estimation. The observation equations with two variables  $\lambda$  and  $\mathbf{x}$  are expressed in two equivalent forms as follows:

$$y(\mathbf{x}, \lambda) = [f_1(\mathbf{x})E(\lambda) \quad f_2(\mathbf{x})C(\lambda)] \begin{bmatrix} S(\lambda) \\ \alpha(\lambda) \end{bmatrix} \quad (5)$$

and

$$y(\mathbf{x}, \lambda) = [S(\lambda)E(\lambda) \quad \alpha(\lambda)C(\lambda)] \begin{bmatrix} f_1(\mathbf{x}) \\ f_2(\mathbf{x}) \end{bmatrix}. \quad (6)$$

Eq. (5) is used for determining the spectral functions when the location weights are fixed. Also Eq. (6) is used for determining the location weights when the spectral functions are fixed. Therefore, minimization of the residual error is performed by estimating the spectral functions and the location weights alternately, based on the linear least square minimization with non-negativity constraints. All estimates are updated in two steps. We repeat this iterative process by starting from Eq.(5) with appropriate initial conditions of the location weighting functions. We also need the initial condition for the spectral function  $C(\lambda)$ .

The spectral functions  $\beta(\lambda)$  and  $C(\lambda)$  are estimated in a separate way without using the iterative algorithm. When the spectral reflectance estimation of  $S(\lambda)$  is updated at each step of the iterative process, the excitation spectrum  $\beta(\lambda)$  and the spectral function  $C(\lambda)$  can be estimated by substituting the reflectance estimate  $\hat{S}(\lambda)$  into the following relationships:

$$\beta(\lambda) = Q(\lambda)(1 - \hat{S}(\lambda)), \quad (7)$$

$$C(\lambda) = \int_{350}^{\lambda} \beta(\lambda)E(\lambda)d\lambda, \quad (8)$$

where  $Q(\lambda)$  is the luminescence efficiency, and the norm of  $\beta(\lambda)$  is defined as  $\|\beta(\lambda)\| = 1$  (see [9]).

In a practical iterative estimation algorithm, we use the initial conditions of a perfect flat surface as  $f_1(\mathbf{x}) = f_2(\mathbf{x}) = 1$  at all  $\mathbf{x}$ , and a constant excitation spectrum as  $\beta(\lambda) = 0.5$ .

In the wavelength range where there is no fluorescent emission of  $\alpha(\lambda) = 0$ , the above observation equations are simplified and reduced to

$$y(\mathbf{x}, \lambda) = f_1(\mathbf{x})S(\lambda)E(\lambda). \quad (9)$$

Therefore, in this range, the spectral reflectance estimate is calculated using all observations and the previously estimated location weight over at entire image region as follows:

$$\hat{S}(\lambda) = \left( \sum_i y(\mathbf{x}_i, \lambda) f_1(\mathbf{x}_i) E(\lambda) \right) / \left( \sum_i f_1^2(\mathbf{x}_i) E^2(\lambda) \right). \quad (10)$$

If multiple light sources rather than one light are available for illuminating the target fluorescent object from the same lighting position, the estimation accuracy of the spectral functions and the location functions is certainly improved. Suppose that  $n$  light sources are available. Then the observation equations by the spectral imaging system for the same fluorescent object are expressed as

$$\begin{bmatrix} y_1(\mathbf{x}, \lambda) \\ y_2(\mathbf{x}, \lambda) \\ \vdots \\ y_n(\mathbf{x}, \lambda) \end{bmatrix} = \begin{bmatrix} f_1(\mathbf{x})E_1(\lambda) & f_2(\mathbf{x})C_1(\lambda) \\ f_1(\mathbf{x})E(\lambda) & f_2(\mathbf{x})C_2(\lambda) \\ \vdots & \vdots \\ f_1(\mathbf{x})E_n(\lambda) & f_2(\mathbf{x})C_n(\lambda) \end{bmatrix} \begin{bmatrix} S(\lambda) \\ \alpha(\lambda) \end{bmatrix} \quad (11)$$

and

$$\begin{bmatrix} y_1(\mathbf{x}, \lambda) \\ y_2(\mathbf{x}, \lambda) \\ \vdots \\ y_n(\mathbf{x}, \lambda) \end{bmatrix} = \begin{bmatrix} S(\lambda)E_1(\lambda) & \alpha(\lambda)C_1(\lambda) \\ S(\lambda)E(\lambda) & \alpha(\lambda)C_2(\lambda) \\ \vdots & \vdots \\ S(\lambda)E_n(\lambda) & \alpha(\lambda)C_n(\lambda) \end{bmatrix} \begin{bmatrix} f_1(\mathbf{x}) \\ f_2(\mathbf{x}) \end{bmatrix}. \quad (12)$$

In this case the above two equations are used for estimating the spectral functions and the location weights alternately, based on the linear least square minimization with non-negativity constraints. The iterative computational procedure and the initial conditions are the same as before.

## Appearance Decomposition and Reconstruction

Figure 2 shows the flow for decomposing the appearance of a fluorescent object and reconstructing the appearance under different illuminant. The iterative algorithm presented in the previous section estimates the Donaldson matrix, constructed with the three spectral functions of reflection, emission, and excitation from the observed spectral image. The algorithm also estimates the location weights for the reflection spectrum and the emission spectrum. The location weights represent the local texture of the object surface. The observed image is decomposed into two textured images of the reflection component and the fluorescent self-luminescent component.

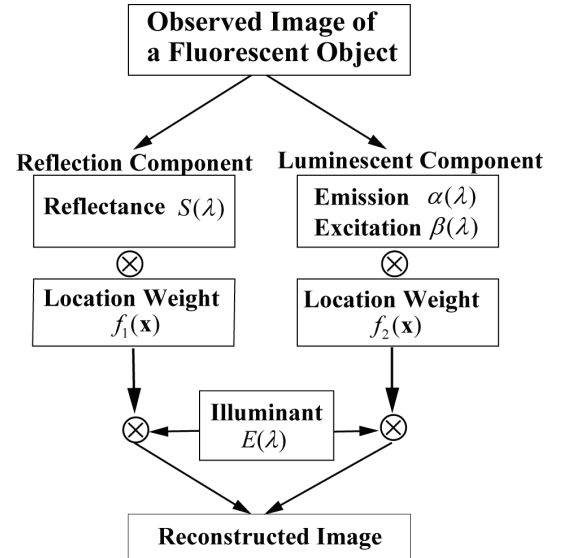


Figure 2. Flow for decomposing the appearance of a fluorescent object and reconstructing the appearance under different illuminant.

Next, we consider appearance reconstruction of the same fluorescent object under different light sources. Let  $\hat{\mathbf{D}}_R$  and  $\hat{\mathbf{D}}_L$

be the estimated reflection component and the luminescent component of the Donaldson matrix, respectively. Also let  $\hat{f}_1(\mathbf{x})$  and  $\hat{f}_2(\mathbf{x})$  be the estimated location weights for the two components. Then the spectral vector observed under an arbitrary illuminant  $\mathbf{e}$  can be predicted by a weighted sum of the two spectral components as follow:

$$\mathbf{y}(\mathbf{x}) = \hat{f}_1(\mathbf{x})\hat{\mathbf{D}}_R\mathbf{e} + \hat{f}_2(\mathbf{x})\hat{\mathbf{D}}_L\mathbf{e} . \quad (13)$$

The above equation means that the two component images are combined into a synthesized image to reconstruct the appearance of the fluorescent object observed under the illuminant  $\mathbf{e}$ . The reflection component  $\hat{\mathbf{D}}_R\mathbf{e}$  depends directly on the illuminant. On the other hand, note that the luminescent component  $\hat{\mathbf{D}}_L\mathbf{e}$  has always the same spectral composition  $\alpha(\lambda)$  independently of the illuminant, although the intensity depends on the illuminant.

### Experimental Results

The spectral imaging system used in the experiments consisted of a monochrome CCD camera (QImaging Retiga 1300) with 12-bit dynamic range and Peltier Cooling, a VariSpec Liquid Crystal Tunable filter (LCTF), and a personal computer. Figure 3 shows the total spectral sensitivity functions of the imaging system, including the filter transmittances and the monochrome camera sensitivity. The spectral images were captured at the equal wavelength intervals of 5 nm. The exposure time of the camera was adjusted according to the total sensitivity function in each channel so that the captured spectral image intensity was equal in every channel. We operated this camera in the visible range [400, 700 nm]. We used two light sources of an incandescent lamp and an artificial sunlight lamp (SERIC XC-100). Figure 4 shows the spectral power distributions for the two light sources.

The feasibility of the proposed method was examined using textured fluorescent samples. The sample were made by painting Acryl Gouache Fluorescent paints on wall papers with rough surface. The size of the samples were 10 cm by 10 cm, which were uniformly illuminated from the vertical direction and photographed from the front with the spectral imaging system. Figures 5 (a) and (b) show the color pictures of the captured spectral images for an orange fluorescent board with a textured surface under the two light sources. The image size is 500 × 500 pixels. We see surface roughness or texture in the captured images.

The proposed algorithm to estimate the spectral functions and the location weights was executed with the initial conditions of  $f_1(\mathbf{x})$  and  $f_2(\mathbf{x})$  being constant and  $\beta(\lambda)$  being constant. The iterative algorithm converged after about three iterations. The average of the residual error  $\|\mathbf{y} - \mathbf{A}\mathbf{f}\|^2$  was 52.2. Figures 6 and 7 show the estimation results of the spectral functions. The solid curves in Figure 6 represent the estimates of  $S(\lambda)$  and  $\alpha(\lambda)$ . The solid curve in Figure 7 represents the estimate of  $\beta(\lambda)$ . The broken curves in both figures represent the estimation results by using the two illuminant projection method [9], where the samples were measured using a spectro-radiometer with the same light sources. In this case, we neglected the texture of the surface and assumed a flat surface without texture. Figure 8 shows the Donaldson matrix of the orange fluorescent object, which was constructed with the estimated spectral functions.

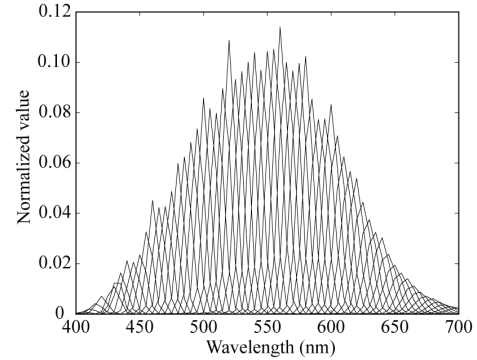


Figure 3. Total spectral sensitivity functions of the imaging system used in experiments.

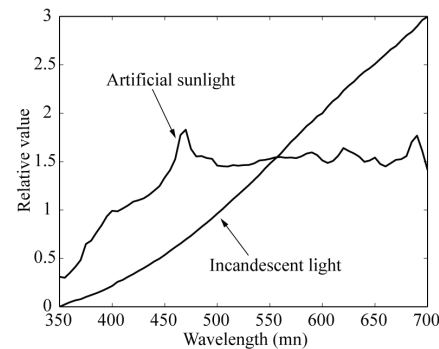
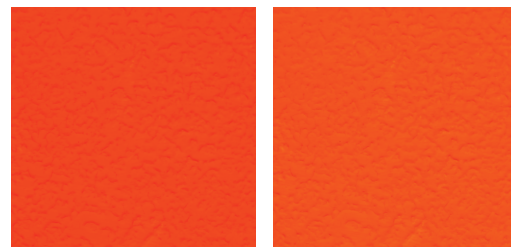


Figure 4. Spectral power distributions of an incandescent light source and an artificial sunlight source used in experiments.



(a) Incandescent light (b) Sunlight

Figure 5. Color pictures of the captured spectral images for an orange fluorescent board with a textured surface under the two light sources.

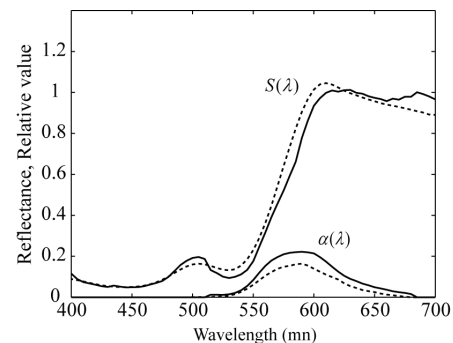


Figure 6. Estimation results for the spectral functions of reflectance and fluorescent emission. The broken curves represent the estimation results by the two illuminant projection method.

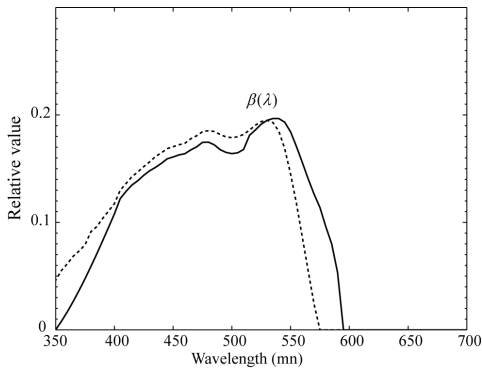


Figure 7. Estimation results for the excitation spectral function. The broken curve represent the estimation results by the two illuminant projection method.

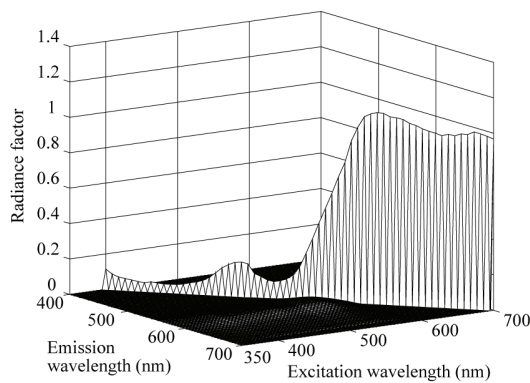


Figure 8. Donaldson matrix constructed with the estimated spectral functions.

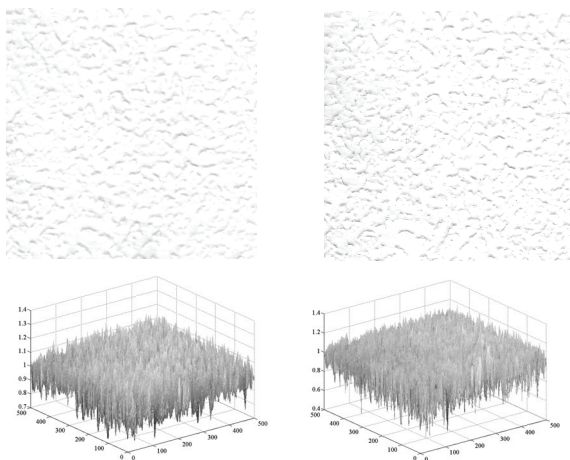


Figure 9. Estimated location weights representing texture patterns. (Left and right: the reflection component and the luminescent component. Upper and lower: the front view and the slant view.)

Figure 9 shows the estimated location weights  $f_1(\mathbf{x})$  and  $f_2(\mathbf{x})$  representing texture patterns for the reflection component and the luminescent component, where the front view and the slant view are depicted for the two components. We can see that, although the texture of the reflection component is similar to the texture of the

fluorescent self-luminescence component, the both textures are not necessarily perfect coincident.

Figures 10 (a) and (b) show the two textured component images of reflection and luminescence based on Figure 2, under the incandescent light and the sunlight. We should note that in Figure 10 (b) the two luminescent component images have the same chromaticity even in different illuminants. Figure 10 (c) shows the reconstructed images of the same object surface under the two light sources by combining the component images (a) and (b). Note that the appearances of the object on the reconstructed images are close to the ones on the original observed image in Figure 5.

Finally, we constructed the appearance of the same fluorescent object surface under different illuminant along the flow in Figure 2. Figures 11 (a) and (b) demonstrate the reflection component image and the luminescent component image for the same object under D65 illuminant. In this image rendering, the spectral power distribution of the D65 light source in X-Rite Macbeth Judge II was used. These were combined into the synthesized image to construct the appearance under D65 as shown in Figure 12 (a). Figure 12 (b) is a real image of the same object observed in the viewing booth of X-Rite Macbeth Judge II. The appearance of the constructed image is very close to the real appearance.

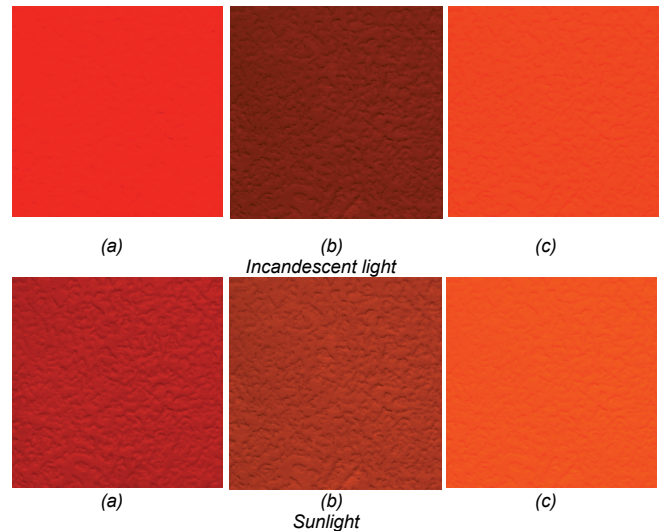


Figure 10. Textured component images (a) and (b) of reflection and luminescence under the incandescent light and the sunlight, and reconstructed images (c) of the same object surface by combining the component images (a) and (b).

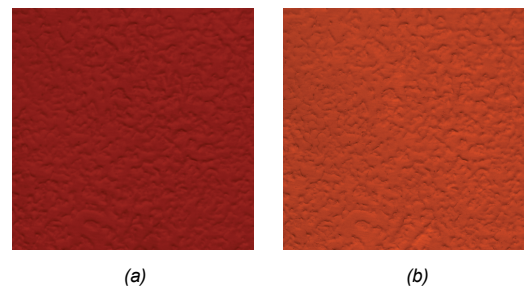


Figure 11. Reflection component image (a) and the luminescent component image (b) for the same object under D65 illuminant.

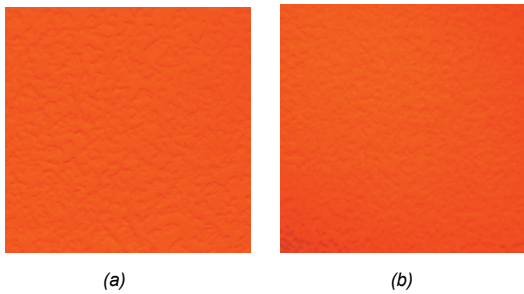


Figure 12. Synthesized image (a) by combining two component images to construct the appearance under D65 and real image (b) of the same object observed in a viewing booth.

## Conclusions

This paper has analyzed the surface appearance of a fluorescent object with textures. The bispectral radiance factor of the fluorescent object was described by the Donaldson matrix. First, we showed that the observed spectral image were modeled by a multiplication of two factors of the spectral functions depending on wavelength and the location weights representing the texture information of the surface. Second, an iterative algorithm was proposed to estimate the spectral reflectance, the bispectral luminescent radiance factor, and the texture information at each pixel point. Third, the observed image was decomposed into two textured images of the reflection component and the luminescent component.

We showed that the realistic appearances of a textured fluorescent object under the arbitrary illumination could be constructed by combining the two component images. The proposed method can be applied to the objects with textured matte surfaces without gloss or highlight. Objects with color texture or curved surface were not considered in this paper. The proposed algorithm estimates the spectral reflectance, the bispectral luminescent radiance factor, and the texture component. This algorithm is stable and fast. With these estimates, the observed images are decomposed into the reflection and luminescent components, and the surface appearance under different illuminant is reconstructed.

This work was supported by JSPS KAKENHI Grant Number JP15H05926 (Grant-in-Aid for Scientific Research on Innovative Areas “Innovative SHITSUKSAN Science and Technology”).

## References

- [1] G. Wyszecki and W. S. Stiles, *Color Science: Concepts and Methods, Quantitative Data and Formulae*. New York: Wiley, 1982.
- [2] J. R. Lakowicz, *Principles of Fluorescence Spectroscopy*, Third ed., Springer, 2006.
- [3] R. Donaldson, Spectrophotometry of fluorescent pigments, *British J. of Applied Physics*, Vol.5, pp.210-214, 1954.
- [4] CIE, *Calibration Methods and Photo-Luminescent Standards for Total Radiance Factor Measurements*, CIE 182:2007, Commission Internationale de l'Eclairage, Vienna, 2007.
- [5] H. Minato, M. Nanjo and Y. Nayatani, Colorimetry and its accuracy in the measurement of fluorescent materials by the two-monochromator method, *Color Res. & Appl.*, Vol.10, pp.84-91, 1985.
- [6] J. Mutanen, *Fluorescent Colors*, Ph.D. Dissertation, Department of Physics, 45, Univ. of Joensuu, 2004.

- [7] E. Allen, Separation of the spectral radiance factor curve of fluorescent substances into reflected and fluorescent components, *Applied Optics*, Vol.12, pp.289-293, 1973.
- [8] M. Mohammadi, *Developing an Imaging Bi-Spectrometer for Fluorescent Materials*, Ph.D. Dissertation, Chester F. Carlson Center for Imaging Science, RIT, 2009.
- [9] S. Tominaga, K. Hirai, and T. Horiuchi, Estimation of bispectral Donaldson matrices of fluorescent objects by using two illuminant projections, *J. Optical Society of America A*, Vol. 32, No. 6, pp.1068-1078, 2015.
- [10] S. Tominaga, K. Kato, K. Hirai, and T. Horiuchi, Bispectral interreflection estimation of fluorescent objects, *Proceedings 23th Color and Imaging Conference (CIC23)*, pp.111-115, 2015.
- [11] S. Tominaga, K. Kato, K. Hirai, and T. Horiuchi, Spectral image analysis of mutual illumination between fluorescent objects, *J. Optical Society of America A*, Vol. 33, No. 8, pp.1476-1487, 2016.
- [12] S. Tominaga, K. Kato, K. Hirai, and T. Horiuchi, Spectral image analysis of fluorescent objects with mutual illumination, *Proceedings 23th Color and Imaging Conference (CIC24)*, pp.59-64, 2016.
- [13] S. Tominaga, K. Kato, K. Hirai, and T. Horiuchi, Spectral image analysis and appearance reconstruction of fluorescent objects under different illuminations, *Proc. 4th CIE Expert Symposium on Colour and Visual Appearance*, pp.140-146, 2016.

## Author Biography

Shoji Tominaga received the B.E., M.S., and Ph.D. degrees in electrical engineering from Osaka University, Japan, in 1970, 1972, and 1975, respectively. In 2006, he joined Chiba University, Japan, where he was a Professor (2006-2013) and Dean (2011-2013) at Graduate School of Advanced Integration Science. He is now a Specially Appointed Researcher, Chiba University. His research interests include digital color imaging, multispectral imaging, and material appearance. He is a Fellow of IEEE, IS&T, SPIE, and OSA.